IEEE Photonics Journal
An IEEE Photonics Society Publication

Open Access

Memory Effect Based Filter to Improve Imaging Quality Through Scattering Layers

Volume 10, Number 5, September 2018

Qianqian Chen
Hexiang He
Xiaoqing Xu
Xiangsheng Xie
Huichang Zhuang
Jianpeng Ye
Yefeng Guan

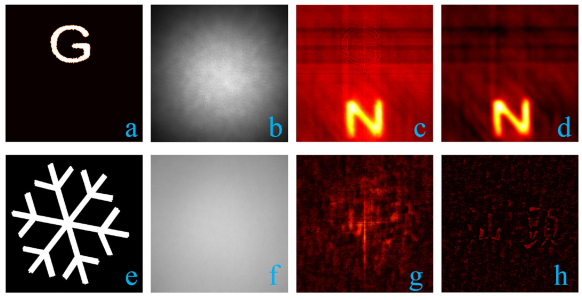

DOI: 10.1109/JPHOT.2018.2873089
1943-0655

IEEE photonics SOCIETY

IEEE

Memory Effect Based Filter to Improve Imaging Quality Through Scattering Layers

Qianqian Chen,[1] **Hexiang He**,[2] **Xiaoqing Xu**,[3] **Xiangsheng Xie**,[1] **Huichang Zhuang**,[3] **Jianpeng Ye**,[1,4] **and Yefeng Guan**[4]

[1]Department of Physics, College of Science, Shantou University, Shantou 515063, China
[2]School of Physics and Optoelectronic Engineering, Foshan University, Foshan 528000, China
[3]School of Physics, Sun Yat-sen University, Guangzhou 510275, China
[4]Guangdong Shunde Innovative Design Institute, Foshan 511447, China

DOI:10.1109/JPHOT.2018.2873089

Manuscript received August 8, 2018; revised September 18, 2018; accepted September 27, 2018. Date of publication October 1, 2018; date of current version October 10, 2018. *(Qianqian Chen and Hexiang He contributed equally to this work.)* Corresponding author: Xiangsheng Xie (e-mail: xxs@stu.edu.cn).

Abstract: Recent extensive studies have promoted the imaging techniques through scattering layers to a reality but the imaging quality still needs to be improved. We demonstrate a high-speed method to image objects hidden behind a thin scattering medium. By analyzing the imaging degradation model of the speckle correlation methods, a memory effect (ME) based filter is proposed to improve the image quality of reconstructed images with deconvolution operation. Comparing to Wiener filter and other related methods, the ME-based filter can optimize the recovered images with the smaller mean square error, suppression of noise background, and central maximum. The proposed ME filter is also applied to improve the imaging method proposed for dynamic imaging through scattering layer with a reference object. The artifact generated by the deviation of retrieved point spread function can be effectively eliminated with a better imaging quality. This ME-based filter is promising to improve the imaging quality for other deconvolution and speckle correlation methods.

Index Terms: Speckle correlation, deconvolution, ME based filter, scattering medium.

1. Introduction

Scatteringis an obstacle in many imaging scenarios because the information carried by the light filed is scrambled. It seems impossible to look through scattering layers or around corners [1] and our sights is blocked by smoke, mist, anisotropy biological tissues, or air turbulence [2]–[4]. However, the information of the objects is not completely lost after scattering [5]. A variety of approaches have been proposed to find such “hidden information” in recent years. Techniques such as wavefront shaping [6]–[10], time-of-flight imaging [11], time reversal or phase conjugation [12]–[21], transmission matrix measurement [22]–[27], holography [28]–[32], and speckle correlation [33]–[47] are demonstrated to effectively recover imaging through scattering media. Among them, speckle correlation method is one of the most promising, as it doesn’t need coherent light sources, raster-scanning, nor wavefront shaping devices. Speckle autocorrelation retrieval [33]–[40] has been exploited to reconstruct objects non-invasively and even a camera phone is qualified for a single-shot reconstruction [34]. Coherent speckle-correlation methods [41], [42] provide field-based information

through thick scattering media. Deconvolution methods [42], [48]–[54] are exploited to demonstrate real-time, 3D, and super resolved imaging. A point source has to be set previously to obtain its speckle, called point spread function (PSF) [56]. Hence the deconvolution method is neither single-shot nor non-invasively. However, the whole imaging system is well presented by the PSF, and the deconvolution method normally turns out a high imaging quality. As a result, deconvolution method is a good tool to analyze scattering phenomena and to explore the corresponding physical mechanisms. For instance, the Field-Of-View (FOV) of the imaging system can be extended to approach the memory effect (ME) range by reducing the applied pupil of the diffuser [48]. It was further enlarged to exceed the ME range with spatial-correlation-achieved PSF [57]. A single-shot monochromatic speckle pattern was adequate for color imaging because deconvolution still works when the spectral overlaps existed [58]. We have recently reported the physical relationships between the speckle patterns of different objects [59], between the PSFs at different depths of object plane [60] and at different wavelengths [61]. Imaging with large FOV, super Depth-Of-Field (DOF), for different objects, at different wavelength, real-time, single-shot and non-invasive has been realized accordingly. It is obviously that better imaging quality will increase the imaging capabilities and enlarge the application scope of the system. Phenomena or physical mechanisms studied through deconvolution method can also be applied to speckle correlation methods and other imaging recovery methods through scattering media.

In this paper, we present a speckle-imaging method to reconstruct incoherently illuminated objects that are hidden behind a thin scattering layer. It is the first time to analyze the noise model of the imaging processing through scattering layer. Thus, a ME based filter is proposed for deconvolution operation by analyzing the image degradation model. The imaging quality is improved markedly after the ME based filter comparing to the conventional inverse filter, Wiener filter, and the novel interferenceless method [55]. The proposed ME filter is also applied to improve the imaging method proposed for dynamic imaging through scattering layer with a reference object [59]. The artefact generated by the deviation of retrieved PSF can be effectively eliminated. Our method has better consistency in restoring the center and edge of objects, and the suppression of noise background is notable as well. The ME based filter is promising to improve the imaging quality for other deconvolution and speckle correlation methods.

2. Experimental Principle

An imaging system, no matter how complicate its internal components are, may be lumped into a single "black box" and be completely described by its PSF. The PSF is shift-invariant within the exit pupil and reduces the object-image relation to a convolution equation. According to the memory effect [62], [63], the speckle patterns from a thin scattering layer will follow the trend of incident light when it is tilted a small angle. So if a thin scattering layer is inserted into a black box, the PSF becomes a speckle pattern and only shift-invariant within a small range of angles (ME range) [1], [62], [63]. By converting the angular shift invariance to lateral shift invariance, the speckle pattern in the imaging plane is superposition of all PSFs from arbitrary point sources from the object. The imaging process can be denoted as a correlation function as [62]–[67],

$$\mathrm{U_i}(x_i, y_i) = F(x_i, y_i) \iint h_I(x_i, y_i; x_o, y_o)\mathrm{U}_o^*(x_o, y_o)dx_o dy_o \tag{1}$$

Where subscripts i and o denote the image and the object plane respectively. $F(x_i, y_i)$ is the form factor function defined as an angular correlation of the emerging speckle patterns of two incident wavefronts with a tilted wavevector $\Delta q_a = k_a - k_{a'}$,

$$F(\Delta q_a) \propto \delta_{\Delta q_a, \Delta q_b} \frac{(\Delta q_a L)^2}{\sinh^2(\Delta q_a L)} \tag{2}$$

The F function has a bell shape curve of angular correlation and is more often referred to as ME range. Imaging process through scattering layers is only valid within this range, leading to a small FOV. However, most of the previous imaging reconstruction methods ignored the F function by

setting $F = 1$ directly. Detailed instructions implied these methods (excepted PSF extending methods [60]) to be effective only within or even much less than the ME range. On the other side, the analysis and classification of noises during imaging is a pending question in speckle correlation methods. The spatial slowly varying envelope of the scattered light pattern was eliminated by dividing the raw imaging data by a low-pass-filter in autocorrelation method [34] and cross-correlation method [31]. The noise-to-signal power ratio (NSPR) is commonly set to be a constant [48], [59]–[61] in deconvolution methods because the present noise models are inadequate to depict the imaging process through diffusers. It is interesting that, although looks disturbing, the speckle pattern is not noise but signal correlated to its tilted angle in ME range. The light intensity of signal pattern under incoherent illumination becomes,

$$I_s(x_i, y_i) = F(x_i, y_i) \iint PSF(x_i, y_i; x_o, y_o)\, O(x_o, y_o)\, dx_o dy_o. \tag{3}$$

When the speckle pattern is almost uniform distribution, the light intensity of evaluated noise would be generated by the degraded PSF (DPSF), and defined as,

$$I_n(x_i, y_i) = [1 - F(x_i, y_i)] \iint DPSF(x_i, y_i; x_o, y_o)\, O(x_o, y_o)\, dx_o dy_o. \tag{4}$$

According to the convolution theorem, the Fourier transformation power spectrum of the undegraded image becomes,

$$S_f = |F\{I_S(x_i, y_i)\}|^2 = \left|\tilde{F} * \left[\widetilde{PSF} \cdot \tilde{O}\right]\right|^2, \tag{5}$$

where $F\{\}$ is a symbol of Fourier transformation. $\tilde{F}$, $\widetilde{PSF}$ and $\tilde{O}$ are 2D Fourier transforms of F, PSF and O respectively.

The Fourier transformation power spectrum of the noise is,

$$S_n = |F\{I_n(x_i, y_i)\}|^2 = \left|\left[\widetilde{DPSF} \cdot \tilde{O}\right] - \tilde{F} * \left[\widetilde{PSF} \cdot \tilde{O}\right]\right|^2. \tag{6}$$

Assuming that PSFs of different object points have similar frequency spectrum envelopes $|\widetilde{PSF}| \approx |\widetilde{DPSF}|$, the noise to signal ratio becomes as,

$$\frac{S_n}{S_f} \approx \frac{\left|1 - \tilde{F}\right|^2}{\left|\tilde{F}\right|^2} \tag{7}$$

To obtain the best excepted image, the restored image in frequency domain can be derived as

$$\tilde{O} = \left[\frac{\left|\widetilde{PSF}\right|^2}{\widetilde{PSF} \cdot \left|\widetilde{PSF}\right|^2 + S_n/S_f}\right] \tilde{I}, \tag{8}$$

where $\tilde{I}$ is 2D Fourier transform of the intensity of speckle pattern I. By introducing (7) into (8), a ME based filter which dedicated to scatter imaging is designed. If the noise is 0 (the noise power spectrum $S_n(x_i, y_i)$ vanishes), the filter will be simplified to an inverse filter. If the term of S_n/S_f is set to be a constant, the filter will be simplified to a wiener filter.

3. Experiment Setup and Results

The experimental setup is shown schematically in Fig. 1. For the deconvolution process, a pinhole with a diameter of 100 μm (or a reference object) is illuminated by an incoherent beam from a light emitting diode (1 W red LED source by Daheng Optics, GCI-060401). The light is transmitted through the scattering layer (Thorlabs, 120 grid ground glass) and the PSF is collected by an image sensor (Basler, ACA2040-90UM). Then the pinhole is replaced by an object (a mask with a specific pattern as shown in Fig. 2) and the speckle pattern is captured by the same CCD. The distance

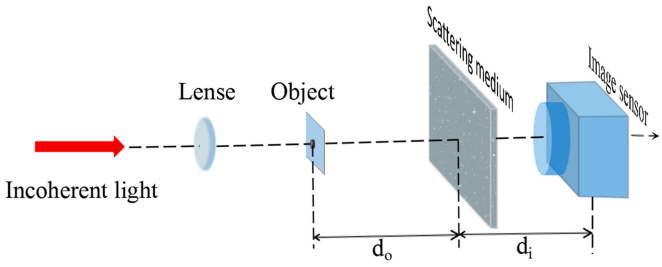

Fig. 1. The schematic of the experimental setup.

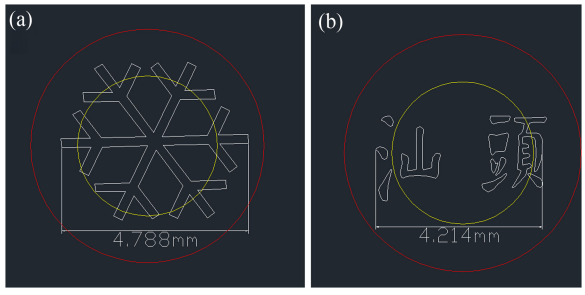

Fig. 2. CAD designed diagram of the tested objects. (a) Snowflake. (b) Chinese characters "汕頭." The red circle and yellow circle indicate the ranges of ME (6.0 mm diameter) and of FOV (3.6 mm diameter) respectively.

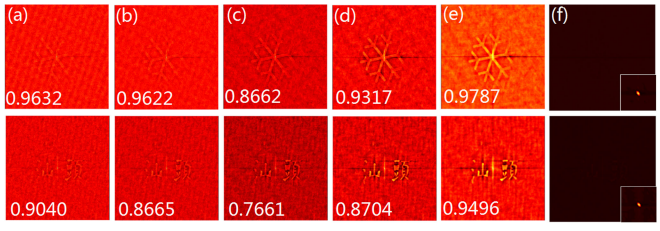

Fig. 3. The reconstructed images of snowflake (first row) and "汕頭" (second row) with Wiener filter by setting NSPR (S_n/S_f) as (a) 0.001, (b) 0.01, (c) 0.1, (d) 1, (e) 10 and (f) 0.1 respectively. The peak values of the central point are setting to as the average of the surrounding pixels except (f). The inserted numbers are the calculated MSEs and the inserted figures in (f) are the 30 enlarge view of the center areas.

from the object plane to the scattering medium (d_o) is 120 mm and that from the scattering medium to the CCD to the scattering media (d_i) is 100 mm.

The CAD designed diagrams of the tested objects are shown in Fig. 2. A snowflake and Chinese characters "汕頭" are used as the patterns ablated by an optical fiber laser marking machine (ML1064-W20, Guangdong Shunde Muller Intelligent Equipment Co., Ltd.) through an aluminum sheet (thickness: 0.17 mm).

The images of the object's shape can be easily retrieved by Wiener filter with the PSF and the speckle pattern, as shown in Fig. 3. Here, mean square error (MSE) index is chosen for evaluating the quality of reconstructed images, which is defined by

$$MSE = \frac{1}{M \cdot N} \sum_{x=0}^{M-1} \sum_{y=0}^{N-1} \left[D(x_i, y_i) - \hat{D}(x_i, y_i) \right]^2, \quad (9)$$

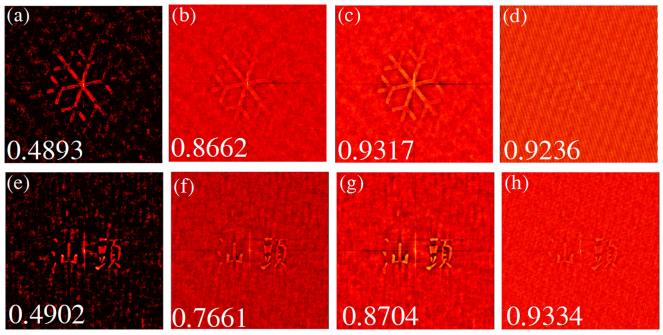

Fig. 4. The reconstructed images of snowflake and "汕頭" with (a) ME base filter, (b) Wiener filter at NSPR = 0.1, (c) Wiener filter at NSPR = 1 and (d) inverse filter. The inserted numbers in (a)–(e) are the calculated MSEs. The peak values of the central area at (b)–(d) are setting to as the average of the surrounding.

where $\hat{D}(x_i, y_i)$ is the reconstructed image, $D(x_i, y_i)$ is the reference image. Every MSE value of "汕頭" images is smaller than that of snowflake. That is because the size of "汕頭" is smaller and the object of "汕頭" has more area within ME range. By setting the NSPR from 0.001 to 10, the smallest MSE is obtained at NSPR = 0.1. Higher NSPR results higher intensity of the central area and background when wide spectrum light source (e.g., LED) is used. In addition, the noise models commonly used in digital image processing (including Wiener filter) are analyzed mostly in frequency domain, including white noise, Gauss noise, Rayleigh noise and so on. There is not a proper model describing the degeneration of the speckle correlation. It is interesting that the noise level of ME based deconvolution changes according to the location deviation of the object point from the reference point, that is, the noise at the center point is almost zero while the NSPR far away from the reference point becomes very large. What's more, the center of the image (Fig. 3(f)) has a quite bright central area, causing the whole picture to be dark and difficult to discern. For visualization, the central area of $5 * 5$ pixels in Fig. 3(a)–(e) has to been artificially setting as the average of the surrounding pixels.

To show the improvement of the proposed method, the reconstructed images of snowflake and "汕頭" of ME based filter, Wiener filter and inverse filter are shown in Fig. 4. The ME based filter is realized by adding a ME based NSPR (Eq. (7)) matrix into the Wiener filter (Eq. 8). Since the F function has a bell shape similar to the Gaussian function, its Fourier transform is also in a bell shape. The NSPR matrix according to Eq. (7) is an inverted bell, in which the values of the central area are almost zero and the values of the outer (supposed to be infinite) are set to be 10. The full weight half maximum (FWHM) of the F function is $ME \times d_i/d_o/s_p = 909$ pixels, where $s_p = 5.5\ \mu$m is the pixel size of the CCD. The imaging quality is boosted after the ME based filtering, which have higher definition and contrast than that of other images. It is worth mentioning that, the peak value of the central area is not exceptional strong. Consequently, the central point suppression operation (averaging of the surrounding pixels applied with Wiener filter) is not necessary in Fig. 4(a) and (e). In comparison, the recovered images of inverse filter are overwhelmed by the background noises (Fig. 4(d) and (h)). The image recovered by Wiener filter looks much better although the background noises are still strong (Fig. 4(b), (c), (f), and (g)).

The cross-sections of the intensity of snowflake in different positions are shown in Fig. 5. Two different positions in Fig. 5(a) are selected for analyzing the experimental results. Fig. 5(b) and (c) show the intensity cross-sections through position 1 and position 2 respectively with three different restored methods mentioned in Fig. 4. The curves of inverse filter are floored in the noise with stronger average intensity. The step curves show that the object edge can be recovered by Wiener filter with different NSPR. Higher NSPR results stronger background intensity. The ME based filter can recover these step curves better with a steeper slope and suppression background, which indicates that the proposed ME based filter method can increasingly enhance the quality of

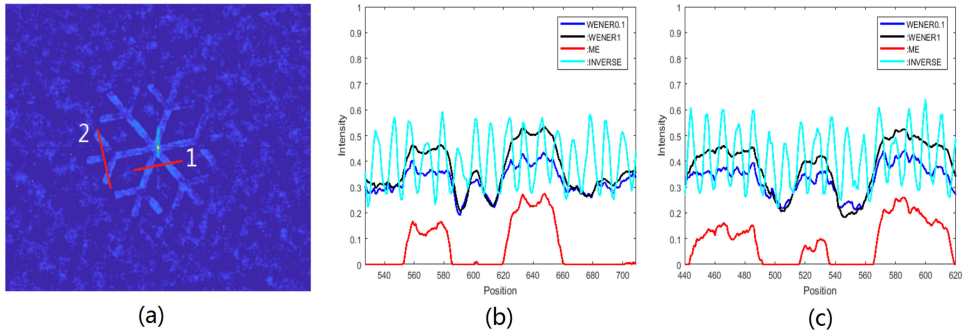

Fig. 5. The cross-sections of the intensity of snowflake. (a) The snowflake image with a position mark. (b) and (c) The intensity cross-section in the position marked with "1" and "2" respectively.

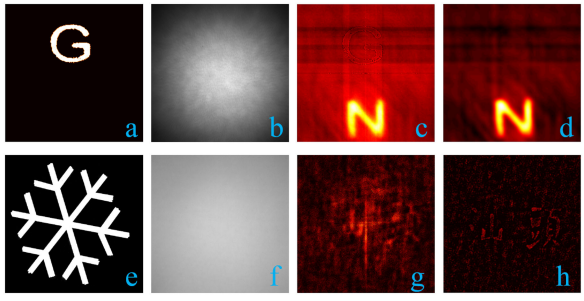

Fig. 6. Imaging through scattering layer with a reference object. (a) and (e) Image binaryzations. (b) and (f) Speckle patterns of the reference objects "G" and snowflake respectively. (c) and (g) Imaging reconstruction with the PSF retrieval method [50] ((a) and (b) was used to reconstruct (c), (e) and (f) was used to reconstruct (g)). (d) and (h) Imaging reconstruction with the ME filter.

restored images. When defining "contrast" as $C_M = (L_H - L_L)/(L_H + L_L)$, where L_H and L_L are the brightest and the darkest values respectively. The C_M values of these four methods are 0.34, 0.48, 1.0, and 0.45 for Weiner0.1, Weiner1, ME based method and Inverse method respectively.

In order to further demonstrate the advantages of the ME based filter in restoration quality improvement, we apply it to the imaging method through scattering layer with a known reference object [59]. It is reported that the PSF of the scattering system can be extracted from a static reference object in a dynamic scene. And the extracted PSF is applied to image other unknown objects in the scene. The process of Ref. [59] is as followed. The image of a reference object (letter "G" about 1 mm high, Fig. 6(a)) and its corresponding speckle pattern through the scattering layer (Fig. 6(b)) were captured previously. An unknown tested object (here is a letter "N") is then replaced (or added adjacent to) the reference object, resulting in a different speckle pattern (not shown here). Using the information of reference object (Fig. 6(a) and (b)), the PSF of the scattering system can be retrieved. The image of the tested object behind the scattering layer is recovered according to the equation of $\widetilde{I_D} = \widetilde{I_R} \times \widetilde{S_M}/\widetilde{S_R}$ [59]. The reconstructed result is shown in Fig. 6(c). One main drawback of this method is that the reconstructed image shows a big artefacts whose shape seems like the shadow of the reference object, even though the reference object was removed ("G" shaped shadow in Fig. 6(c)). It is because the correlation of the speckle patterns from different object points is degraded, so that the retrieved PSF is deviated from the real PSF and the artefacts is generated. Actually, the PSF retrieval process in this paper can be simplified into a deconvolution. According to Eq. (3) and (4), the speckle pattern I contains DPSF while the object has a perfect imaging O as a known shape. Hence the shape information of the known object is added into the retrieved PSF. This problem can be solved by applying the proposed ME based filter the PSF retrieval process. Multiplying O by the F function, the degradation in correlation adds to the object and the

retrieval PSF would not contain any information of the known object. And finally, the quality of the reconstructed image improves a lot and the artifacts related to the reference object is removed (Fig. 6(d)).

Another example is shown in Fig. 6(e)–(h). Here a scene with larger objects is tested. The snowflake is used as the reference object (Fig. 6(e)) and mask of "汕頭" is as the test object. The restored result with method reported in Ref. [59] is shown in Fig. 6(g). It is obvious that the shadow of the snowflake cannot be removed, which leads to a messy pattern. In comparison, by applying the proposed ME based filter twice (PSF retrieval and imaging reconstruction), the quality of restored image improves a lot. As it is shown in Fig. 6(h), the shape of "汕頭" can be clearly resolved.

4. Discussion

In addition, the novel interfereless method [55] is tested for comparison in the same way, the best MSEs of snowflake and "汕頭" are 0.6786 and 0.6972 respectively. The MSE vs. γ curve is similar to the curve in literature, but the optimization point is offset to $\gamma = 0.6$. The reason for this deviation may be that the tested objects is larger, almost filled the ME range, and the spectral width in the paper is larger. Unlike Wiener filter needs to adjust a wide range of NSPR, the best γ value is easy to be found with the interfereless method.

The FOV in Fig. 2 is obviously smaller than the ME range, which cannot meet the simple equation of ME $=$ FOV/R [30], where R is the object distance. Because the CCD has a limited sensor area and can only capture part of the correlated speckles. If the speckle halo is partially captured, it will results in a smaller FOV compared with the theoretical limitation. To enlarge the system's FOV, a demagnifying lenses system was suggested to be introduced [48]. If the speckle halo can be fully captured, the FOV angle can approach to the ME range. Moreover, there are several methods to improve the quality of the reconstructed images in experiment by taking into account the ME range. Since the deconvolution methods are based on an assumption that scattering medium is a linear shift-invariant system. A paraxial target with small size or a scatter layer with large ME range would satisfy to this assumption better. Narrower bandwidth of the illuminating light source and sparsity of the objects result a better speckle contrast [66]. A laser (i.e., He-Ne) passing through a rotating diffuser is often used as the light source benefited from its high speckle contrast. On the other side, if the dynamic range of the CCD is high enough and the readout noise is low enough, the influence of low speckle contrast can be ignored. The speckle contrast can be increased with a larger size of speckle pattern. By placing a diaphragm before the diffuser to reduce its effective area, the speckle pattern will obviously be enlarged. Inserting a lens (e.g., objective lens) close to the diffuser (within its focal length) can also limit the effective area of the diffuser with the small entrance pupil of the objective lens.

The proposed ME based filtering introduces a filter, which varies in space. It is promising fit to the actual scattering process and can be revealed the correct NSPR when doing deconvolution restoration. The ME based filtering method can vastly suppress the central disturbance comparing to other normal methods mentioned in this paper. So that it can help to expand the application of deconvolution scattering imaging technique, especially for situation when the tested object contains fine structure in the imaging center. By introducing the ME based filtering, the time consumption of the image reconstruction processing only increases a little [48]. It takes about 1.1 ms for a single image (2048×2048 pixels) reconstruction by a commercial GPU (NVIDIA GTX 970) (corresponding to a frame rate of 0.9 kHz) with the advantages of parallel computing.

5. Conclusion

In conclusion, we demonstrate a high-quality method to image objects through a thin scattering medium with ME filtering. The proposed method of the ME based filter has better consistency in restoring the center and edge of objects, and the effect of background suppression is notable. We believe it is more close to the real scattering situation by considering the noise model of the scattering

process when doing deconvolution imaging calculation. The proof-of-concept experiment for the proposed method can be carried out under incoherent optical system. Therefore, the requirements of good coherence source and precisely alignment are not as strict as the case of coherence optical system. Furthermore, the scattering medium chosen in this paper are a common scattering layer with inhomogeneous structure and strong ability to scatter light. So that it can be replaced with some natural scatter media such as human skin, tissues, fog and other turbid media. Accordingly, our method can be easily expanded to a variety of applications with different complex environments. The proposed ME based filter is promising to improve the imaging quality for all deconvolution and speckle correlation methods. By improving the restoration quality a bit step, we hope this method can push the applications of decovolution scattering imaging a bit step.

Acknowledgment

The authors would like to thank A. P. Mosk for his useful discussions.

References

[1] I. Freund, "Looking through walls and around corners," *Physica A*, vol. 168, no. 1, pp. 49–65, 1990.
[2] A. P. Mosk, A. Lagendijk, G. Lerosey, and M. Fink, "Controlling waves in space and time for imaging and focusing in complex media," *Nat. Photon.*, vol. 6, no. 5, pp. 283–292, 2012.
[3] V. Tuchin, *Tissue Optics: Light Scattering Methods and Instruments for Medical Diagnosis*, 2nd ed. Bellingham, WA, USA: SPIE, vol. 13, 2007.
[4] M. Gu, X. Gan, and X. Deng, *Microscopic Imaging Through Turbid Media*. Berlin, Germany: Springer-Verlag, 2015.
[5] P. S. Idell, J. Knopp, J. D. Gonglewski, and D. G. Voelz, "Image synthesis from nonimaged laser-speckle patterns: Experimental verification," *Opt. Lett.*, vol. 14, no. 3, pp. 154–156, 1989.
[6] I. M. Vellekoop and A. P. Mosk, "Focusing coherent light through opaque strongly scattering media," *Opt. Lett.*, vol. 32, no. 16, pp. 2309–2311, 2007.
[7] O. Katz, E. Small, and Y. Silberberg, "Looking around corners and through thin turbid layers in real time with scattered incoherent light," *Nat. Photon.*, vol. 6, no. 6, pp. 549–553, 2012.
[8] H. He, Y. Guan, and J. Zhou, "Image restoration through thin turbid layers by correlation with a known object," *Opt. Exp.*, vol. 21, no. 10, pp. 12539–12545, 2013.
[9] I. M. Vellekoop, "Feedback-based wavefront shaping," *Opt. Exp.*, vol. 23, no. 9, pp. 12189–12206, 2015.
[10] R. Horstmeyer, H. Ruan, and C. Yang, "Guidestar-assisted wavefront-shaping methods for focusing light into biological tissue," *Nat. Photon.*, vol. 9, no. 9, pp. 563–571, 2015.
[11] A. Velten, T. Willwacher, O. Gupta, A. Veeraraghavan, M. Bawendi, and R. Raskar, "Recovering three dimensional shape around a corner using ultra-fast time-of-flight imaging," *Nat. Commun.*, vol. 3, no. 2, 2012, Art. no. 745.
[12] Z. Yaqoob, D. Psaltis, M. S. Feld, and C. Yang, "Optical phase conjugation for turbidity suppression in biological samples," *Nat. Photon.*, vol. 2, no. 2, pp. 110–115, 2008.
[13] C.-L. Hsieh, Y. Pu, R. Grange, G. Laporte, and D. Psaltis, "Imaging through turbid layers by scanning the phase conjugated second harmonic radiation from a nanoparticle," *Opt. Exp.*, vol. 18, no. 20, pp. 20723–20731, 2010.
[14] X. Yang, C.-L. Hsieh, Y. Pu, and D. Psaltis, "Three-dimensional scanning microscopy through thin turbid media," *Opt. Exp.*, vol. 20, no. 3, pp. 2500–2506, 2012.
[15] K. Si, R. Fiolka, and M. Cui, "Fluorescence imaging beyond the ballistic regime by ultrasound pulse guided digital phase conjugation," *Nat. Photon.*, vol. 6, no. 10, pp. 657–661, 2012.
[16] Y. M. Wang, B. Judkewitz, C. A. DiMarzio, and C. Yang, "Deep-tissue focal fluorescence imaging with digitally time-reversed ultrasound-encoded light," *Nat. Commun.*, vol. 3, 2012, Art. no. 928.
[17] C. Ma, X. Xu, Y. Liu, and L. Wang, "Time-reversed adapted-perturbation (TRAP) optical focusing onto dynamic objects inside scattering media," *Nat. Photon.*, vol. 8, no. 12, pp. 931–936, 2014.
[18] K. Wu, Q. Cheng, Y. Shi, H. Wang, and G. P. Wang, "Hiding scattering layers for noninvasive imaging of hidden objects," *Sci. Rep.*, vol. 5, 2015, Art. no. 8375.
[19] I. N. Papadopoulos, J. Jouhanneau, J. F. A. Poulet, and B. Judkewitz, "Scattering compensation by focus scanning holographic aberration probing (F-SHARP)," *Nat. Photon.*, vol. 11, no. 2, pp. 116–123, 2017.
[20] H. He and K. Wong, "An improved wavefront determination method based on phase conjugation for imaging through thin scattering medium," *J. Opt.*, vol. 18, no. 8, 2016, Art. no. 085604.
[21] S. H. Tseng, "Investigating the optical phase conjugation reconstruction phenomenon of light multiply scattered by a random medium," *IEEE Photon. J.*, vol. 2, no. 4, pp. 636–641, Aug. 2010.
[22] S. Popoff, G. Lerosey, M. Fink, A. C. Boccara, and S. Gigan, "Image transmission through an opaque material," *Nat. Commun.*, vol. 1, no. 6, 2010, Art. no. 81.
[23] S. M. Popoff, G. Lerosey, R. Carminati, M. Fink, A. C. Boccara, and S. Gigan, "Measuring the transmission matrix in optics: An approach to the study and control of light propagation in disordered media," *Phys. Rev. Lett.*, vol. 104, no. 10, 2010, Art. no. 100601.
[24] Y. Choi *et al.*, "Scanner-free and wide-field endoscopic imaging by using a single multimode optical fiber," *Phys. Rev. Lett.*, vol. 109, no. 20, 2012, Art. no. 203901.

[25] M. Kim, W. Choi, Y. Choi, C. Yoon, and W. Choi, "Transmission matrix of a scattering medium and its applications in biophotonics," *Opt. Exp.*, vol. 23, no. 10, pp. 12648–12668, 2015.
[26] Y. Zhao, Q. Chen, S. Zhou, G. Gu, and X. Sui, "Super-resolution imaging through scattering medium based on parallel compressed sensing," *IEEE Photon. J.*, vol. 9, no. 5, Oct. 2017, Art. no. 7803012.
[27] Y. Zhou and X. Li, "Optimization of iterative algorithms for focusing light through scattering media," *IEEE Photon. J.*, vol. 9, no. 2, Apr. 2017, Art. no. 6100310.
[28] W. Harm, C. Roider, A. Jesacher, S. Bernet, and M. Ritsch-Marte, "Lensless imaging through thin diffusive media," *Opt. Exp.*, vol. 22, no. 18, pp. 22146–22156, 2014.
[29] A. K. Singh, D. N. Naik, G. Pedrini, M. Takeda, and W. Osten, "Looking through a diffuser and around an opaque surface: a holographic approach," *Opt. Exp.*, vol. 22, no. 7, pp. 7694–7701, 2014.
[30] S. Li and J. Zhong, "Dynamic imaging through turbid media based on digital holography," *J. Opt. Soc. Amer.*, vol. 31, no. 3, pp. 480–486, 2014.
[31] A. K. Singh, D. N. Naik, G. Pedrini, M. Takeda, and W. Osten, "Exploiting scattering media for exploring 3D objects," *Light Sci. Appl.*, vol. 6, 2017, Art. no. e16219.
[32] A. Ozcan, H. Günaydin, X. Lin, Y. Rivenson, and Y. Zhang, "Extended depth-of-field in holographic imaging using deep-learning-based autofocusing and phase recovery," *Optica*, vol. 5, pp. 704–710, 2018.
[33] J. Bertolotti, E. G. van Putten, C. Blum, A. Lagendijk, W. L. Vos, and A. P. Mosk, "Non-invasive imaging through opaque scattering layers," *Nature*, vol. 491, no. 7423, pp. 232–234, 2012.
[34] O. Katz, P. Heidmann, M. Fink, and S. Gigan, "Non-invasive single-shot imaging through scattering layers and around corners via speckle correlations," *Nat. Photon.*, vol. 8, no. 10, pp. 784–790, 2014.
[35] K. T. Takasaki and J. W. Fleischer, "Phase-space measurement for depth-resolved memory-effect imaging," *Opt. Exp.*, vol. 22, no. 25, pp. 31426–31433, 2014.
[36] E. Edrei and G. Scarcelli, "Optical imaging through dynamic turbid media using the Fourier-domain shower-curtain effect," *Optica*, vol. 3, no. 1, pp. 71–74, 2016.
[37] Y. Shi, Y. Liu, J. Wang, and T. Wu, "Non-invasive depth-resolved imaging through scattering layers via speckle correlations and parallax," *Appl. Phys. Lett.*, vol. 110, no. 23, 2017, Art. no. 231101.
[38] T. Wu, O. Katz, X. Shao, and S. Gigan, "Single-shot diffraction-limited imaging through scattering layers via bispectrum analysis," *Opt. Lett.*, vol. 41, no. 21, pp. 5003–5006, 2016.
[39] M. Cua, E. Zhou, and C. Yang, "Imaging moving targets through scattering media," *Opt. Exp.*, vol. 25, no. 4, pp. 3935–3945, 2017.
[40] M. Hofer, C. Soeller, S. Brasselet, and J. Bertolotti, "Wide field fluorescence epi-microscopy behind a scattering medium enabled by speckle correlations," *Opt. Exp.*, vol. 26, no. 8, pp. 9866–9881, 2018.
[41] J. A. Newman and K. J. Webb, "Imaging optical fields through heavily scattering media," *Phys. Rev. Lett.*, vol. 113, no. 26, 2014, Art. no. 263903.
[42] J. A. Newman, Q. Luo, and K. J. Webb, "Imaging hidden objects with spatial speckle intensity correlations over object position," *Phys. Rev. Lett.*, vol. 116, no. 7, 2016, Art. no. 073902.
[43] Y. Hu, X. Jin, K. Wei, and Q. Dai, "Imaging through scattering media with intensity modulated incoherent sources," in *Proc. 2016 IEEE Int. Conf. Image Process.*, 2016, pp. 1729–1733.
[44] Y. S. Baek, K. R. Lee, and Y. K. Park, "High-resolution long-working-distance reference-free holographic microscopy exploiting speckle-correlation scattering matrix," arXiv: 1802.10321, 2018.
[45] Z. Lei, C. Wang, D. Zhang, L. Wang, and W. Gong, "Second-order intensity-correlated imaging through the scattering medium," *IEEE Photon. J.*, vol. 9, no. 6, Dec. 2017, Art. no. 7500207.
[46] F. Shen, B. Zhang, K. Guo, Z. Yin, and Z. Guo, "The depolarization performances of the polarized light in different scattering media systems," *IEEE Photon. J.*, vol. 10, no. 2, Apr. 2018, Art. no. 3900212.
[47] H. Hu, L. Zhao, X. Li, H. Wang, and T. Liu, "Underwater image recovery under the non-uniform optical field based on polarimetric imaging," *IEEE Photon. J.*, vol. 10, no. 1, Feb. 2018, Art. no. 6900309.
[48] H. Zhuang, H. He, X. Xie, and J. Zhou, "High speed color imaging through scattering media with a large field of view," *Sci. Rep.*, vol. 6, 2016, Art. no. 32696.
[49] E. Edrei and G. Scarcelli, "Memory-effect based deconvolution microscopy for super-resolution imaging through scattering media," *Sci. Rep.*, vol. 6, 2016, Art. no. 33558.
[50] S. K. Sahoo, D. Tang, and C. Dang, "Single-shot multispectral imaging with a monochromatic camera," *Optica*, vol. 4, no. 10, pp. 1209–1213, 2017.
[51] R. French, S. Gigan, and O. L. Muskens, "Speckle-based hyperspectral imaging combining multiple scattering and compressive sensing in nanowire mats," *Opt. Lett.*, vol. 42, no. 9, pp. 1820–1823, 2017.
[52] S. Lee, K. Lee, S. Shin, and Y. Park, "Generalized image deconvolution by exploiting the transmission matrix of an optical imaging system," *Sci. Rep.*, vol. 7, no. 1, 2017, Art. no. 8961.
[53] N. Antipa *et al.*, "DiffuserCam: Lensless single-exposure 3D imaging," *Optica*, vol. 5, no. 1, pp. 1–9, 2018.
[54] A. K. Singh, D. N. Naik, G. Pedrini, M. Takeda, and W. Osten, "Exploiting scattering media for exploring 3D objects," *Light Sci. Appl.*, vol. 6, no. 2, 2017, Art. no. e16219.
[55] S. Mukherjee, A. Vijayakumar, M. Kumar, and J. Rosen, "3D imaging through scatterers with interferenceless optical system," *Sci. Rep.*, vol. 8, no. 1, 2018, Art. no. 1134.
[56] X. Xie, Y. Chen, K. Yang, and J. Zhou, "Harnessing the point-spread function for high-resolution far-field optical microscopy," *Phys. Rev. Lett.*, vol. 113, no. 26, 2014, Art. no. 263901.
[57] L. Li, Q. Li, S. Sun, H. Z. Lin, W. T. Liu, and P. X. Chen, "Imaging through scattering layers exceeding memory effect range with spatial-correlation-achieved point-spread-function," *Opt. Lett.*, vol. 43, no. 8, pp. 1670–1673, 2018.
[58] S. K. Sahoo, D. Tang, and C. Dang, "Single-shot multispectral imaging with a monochromatic camera," *Optica*, vol. 4, no. 10, pp. 1209–1213, 2017.
[59] X. Xu *et al.*, "Imaging objects through scattering layers and around corners by retrieval of the scattered point spread function," *Opt. Exp.*, vol. 25, no. 26, pp. 32829–32840, 2017.

[60] X. Xie *et al.*, "Extended depth-resolved imaging through a thin scattering medium with PSF manipulation," *Sci. Rep.*, vol. 8, no. 1, 2018, p. 4585.
[61] X. Xu *et al.*, "Imaging of objects through a thin scattering layer using a spectrally and spatially separated reference," *Opt. Exp.*, vol. 26, no. 12, pp. 15073–15083, 2018.
[62] I. Freund, M. Rosenbluh, and S. Feng, "Memory effects in propagation of optical waves through disordered media," *Phys. Rev. Lett.*, vol. 61, no. 20, pp. 2328–2331, 1988.
[63] S. Feng, C. Kane, P. A. Lee, and A. D. Stone, "Correlations and fluctuations of coherent wave transmission through disordered media," *Phys. Rev. Lett.*, vol. 61, no. 7, pp. 834–837, 1988.
[64] S. Schott, J. Bertolotti, J. F. Leger, L. Bourdieu, and S. Gigan, "Characterization of the angular memory effect of scattered light in biological tissues," *Opt. Exp.*, vol. 23, no. 10, pp. 13505–13516, 2015.
[65] N. Antipa, S. Necula, N. Ren, and L. Waller, "Single-shot diffuser-encoded light field imaging," in *Proc. 2016 IEEE Int. Conf. Comput. Photography*, 2016, pp. 1–11.
[66] J. W. Goodman, *Speckle Phenomena in Optics: Theory and Applications*. Greenwood Village, CO, USA: Roberts & Co., 2007.
[67] Z. Yang *et al.*, "Digital spiral object identification using random light," *Light Sci. Appl.*, vol. 6, no. 7, 2017, Art. no. e17013.